

Searches for lepton flavour and lepton number violation in K^+ decays

Angela Romano*[†]

University of Birmingham

E-mail: angela.romano@cern.ch

The NA62 experiment at CERN offers the highest experimental sensitivity to rare and forbidden kaon decays. A search for lepton number violating processes $K^+ \rightarrow \pi^- e^+ e^+$ and $K^+ \rightarrow \pi^- \mu^+ \mu^+$, using a partial data set collected by NA62 in 2016-2018, is reported. No signals are observed and upper limits at 90% confidence level on the branching fractions of these decays are obtained: 2.2×10^{-10} and 4.2×10^{-11} , respectively. These results improve on previously reported measurements by factors of 3 and 2, respectively.

*European Physical Society Conference on High Energy Physics - EPS-HEP2019 -
10-17 July, 2019
Ghent, Belgium*

*Speaker.

[†]for the NA62 Collaboration: R. Aliberti, F. Ambrosino, R. Ammendola, B. Angelucci, A. Antonelli, G. Anzivino, R. Arcidiacono, T. Bache, M. Barbanera, J. Bernhard, A. Biagioni, L. Bician, C. Biino, A. Bizzeti, T. Blazek, B. Bloch-Devaux, V. Bonaiuto, M. Boretto, M. Bragadireanu, D. Britton, F. Brizioli, M.B. Brunetti, D. Bryman, F. Bucci, T. Cappella, J. Carmignani, A. Ceccucci, P. Cenci, V. Cerny, C. Cerri, B. Checcucci, A. Conovaloff, P. Cooper, E. Cortina Gil, M. Corvino, F. Costantini, A. Cotta Ramusino, D. Coward, G. D'Agostini, J. Dainton, P. Dalpiaz, H. Danielsson, N. De Simone, D. Di Filippo, L. Di Lella, N. Doble, B. Dobrich, F. Duval, V. Duk, J. Engelfried, T. Enik, N. Estrada-Tristan, V. Falaleev, R. Fantechi, V. Fascianelli, L. Federici, S. Fedotov, A. Filippi, M. Fiorini, J. Fry, J. Fu, A. Fucci, L. Fulton, E. Gamberini, L. Gatignon, G. Georgiev, S. Ghinescu, A. Gianoli, M. Giorgi, S. Giudici, F. Gonnella, E. Goudzovski, C. Graham, R. Guida, E. Gushchin, F. Hahn, H. Heath, E.B. Holzer, T. Husek, O. Hutanu, D. Hutchcroft, L. Iacobuzio, E. Iacopini, E. Imbergamo, B. Jenninger, J. Jerhot, R.W. Jones, K. Kampf, V. Kekelidze, S. Kholodenko, G. Khorauli, A. Khotyantsev, A. Kleimenova, A. Korotkova, M. Koval, V. Kozhuharov, Z. Kucerova, Y. Kudenko, J. Kunze, V. Kurochka, V. Kurshetsov, G. Lanfranchi, G. Lamanna, E. Lari, G. Latino, P. Laycock, C. Lazzeroni, M. Lenti, G. Lehmann Miotto, E. Leonardi, P. Lichard, L. Litov, R. Lollini, D. Lomidze, A. Lonardo, P. Lubrano, M. Lupi, N. Lurkin, D. Madigozhin, I. Mannelli, G. Mannocchi, A. Mapelli, F. Marchetto, R. Marchevski, S. Martellotti, P. Massarotti, K. Massri, E. Maurice, M. Medvedeva, A. Mefodev, E. Menichetti, E. Migliore, E. Minucci, M. Mirra, M. Mishva, N. Molokanova, M. Moulson, S. Movchan, M. Napolitano, I. Neri, F. Newson, A. Norton, M. Noy, T. Numao, V. Obraztsov, A. Ostankov, S. Padolski, R. Page, V. Palladino, A. Parenti, C. Parkinson, E. Pedreschi, M. Pepe, M. Perrin-Terrin, L. Peruzzo, P. Petrov, Y. Petrov, F. Petrucci, R. Piandani, M. Piccini, J. Pinzino, I. Polenkevich, L. Pontisso, Yu. Potrebenikov, D. Protopopescu, M. Raggi, A. Romano, P. Rubin, G. Ruggiero, V. Ryjov, A. Salamon, C. Santoni, G. Saracino, F. Sargeni, S. Schuchmann, V. Semenov, A. Sergi, A. Shaikhiev, S. Shkarovskiy, D. Soldi, V. Sugonyaev, M. Sozzi, T. Spadaro, F. Spinella, A. Sturgess, J. Swallow, S. Trilov, P. Valente, B. Velghe, S. Venditti, P. Vicini, R. Volpe, M. Vormstein, H. Wahl, R. Wanke, B. Wrona, O. Yushchenko, M. Zamkovsky, A. Zinchenko.

1. Introduction

The conservation of lepton number and lepton flavour are properties of the Standard Model (SM) not explicitly required during its construction. Many scenarios beyond SM predict the existence of lepton number violating (LNV) and/or lepton flavour violating (LFV) processes. For example, the decays of the charged kaon $K^+ \rightarrow \pi^- l^+ l^+$ (with $l = e, \mu$) violate the conservation of lepton number by two units, and may be mediated by a massive Majorana neutrino [1, 2]. The observation of such processes would be a clear indication of physics beyond the SM description. The world knowledge (prior to the reported analysis) for these decays is based on the following upper limits at 90% confidence level on their branching fractions: $B(K^+ \rightarrow \pi^- e^+ e^+) < 6.4 \times 10^{-10}$ obtained by the BNL E865 experiment [3], and $B(K^+ \rightarrow \pi^- \mu^+ \mu^+) < 8.6 \times 10^{-11}$ obtained by the CERN NA48/2 experiment [4]. A search for $K^+ \rightarrow \pi^- l^+ l^+$ (with $l = e, \mu$) with about 30% of the data collected by the NA62 experiment at CERN in 2016-18 is reported here.

2. The NA62 experiment at CERN

The NA62 experiment [5] at the CERN Super Proton Synchrotron (SPS) is a fixed-target detector designed for the study of rare kaon decays. It represents the current kaon physics programme at CERN and offers a timely and complementary approach, with respect to direct and indirect searches at the Large Hadron Collider, to probe new physics at short distances corresponding to energy scales up to 100 TeV. The NA62 primary goal is the precise measurement of the ultra-rare $K^+ \rightarrow \pi^+ \nu \bar{\nu}$ decay, using a decay-in-flight technique, novel for this channel. In the SM the expected probability for this decay is about 10^{-10} . Owing to the strong suppression in the SM, the $K^+ \rightarrow \pi^+ \nu \bar{\nu}$ decay is sensitive to beyond SM scenarios [6, 7], probing the highest energy scales accessible amongst rare meson decays. After a decade of intense development and construction, NA62 has collected physics data in 2016-2018. The statistics of the first sample, collected with the full detector in 2016, allowed NA62 to reach the domain of 10^{-10} single event sensitivity for the $K^+ \rightarrow \pi^+ \nu \bar{\nu}$ decay and validated the novel experimental technique [8].

The NA62 high intensity beam flux and detector performances [5] provide unprecedented background suppression and precision measurement capabilities, and can be exploited to expand the physics scope of the experiment. So despite being built for a specific goal, NA62 presents a broad and competitive physics programme in kaon decays and beyond. In addition to $K^+ \rightarrow \pi^+ \nu \bar{\nu}$ the programme includes: precision tests of lepton flavour universality (LFU) and chiral perturbation theory (ChPT); precision measurement of rare decays, like $K \rightarrow \pi ll$, $K^+ \rightarrow \pi^+ \gamma l^+ l^-$ and $K^+ \rightarrow l^+ \nu \gamma$ with $l = e, \mu$; searches for forbidden lepton flavour/number violating (LFV/LNV) processes in K^+ and π^0 decays, like $K^+ \rightarrow \pi^- l^+ l^+$ with $l = e, \mu$ (reported in this contribution) or $\pi^0 \rightarrow e \mu$; searches for hidden-sector particles, such as heavy neutral lepton and dark photons [9].

The beam and detector The NA62 detector is shown in Fig. 1 and is explained in detail in [5]. A secondary unseparated hadron beam of central momentum (75 ± 0.8) GeV/ c is produced from SPS primary protons at 400 GeV/ c directed on a beryllium target. The total particle rate at nominal intensity is about 750 MHz and the main beam components correspond to $\sim 70\%$ of π^+ , $\sim 6\%$ of K^+ and $\sim 24\%$ of protons. About 10% of K^+ decays in a fiducial volume (FV) contained in a large vacuum cylindrical tank kept at 10^{-6} mbar pressure, to minimise the multiple scattering of the decay

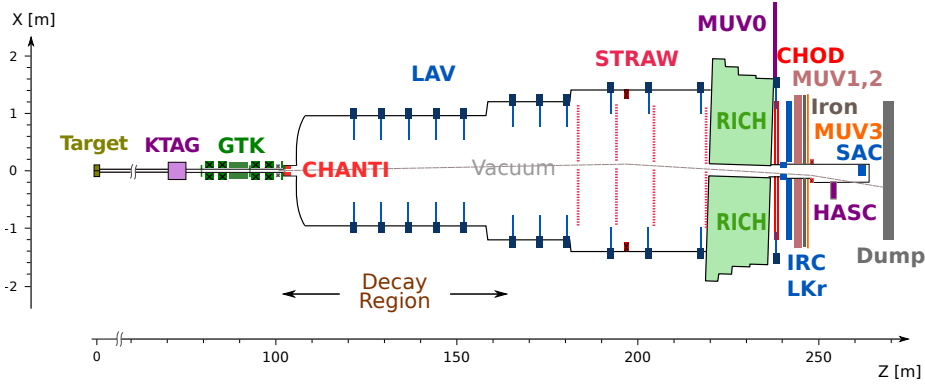


Figure 1: Schematic layout of the NA62 experiment in the xz plane.

products, and the number of interactions of the beam with the residual gas. The NA62 tracking system is composed by three stations of silicon micro-pixel GigaTracKer (GTK) beam spectrometer and four straw chambers spectrometer (STRAW) responsible for the detection and tracking of particles upstream and downstream the FV, respectively. The NA62 particle identification (PID) strategy relies on a Cherenkov differential counter (KTAG) for the positive identification of kaons upstream the FV, a Ring Imaging Cherenkov (RICH) detector for $\pi/\mu/e$ identification and timing, a liquid Krypton (LKr) electromagnetic calorimeter and hadronic calorimeters (MUV1,2). The NA62 photon veto system is composed by several detectors covering different photon emission angle regions: LKr, intermediate (IRC) and small angle (SAC) calorimeters responsible for the rejection of photons emitted in the forward region (up to 15 mrad), 12 stations of large angle vetoes (LAV), distributed over the length of the decay tank, for photons emitted at large angle (15-50 mrad). The veto system also comprises plastic scintillators (MUV0, MUV3) to suppress muons.

3. Data samples and event selections

Searches for two LNV modes $K^+ \rightarrow \pi^- e^+ e^+$ and $K^+ \rightarrow \pi^- \mu^+ \mu^+$ using a subset (equivalent to 3 months) of 2017 data are reported. A blind analysis strategy is adopted, and the corresponding SM flavour changing neutral current (FCNC) $K^+ \rightarrow \pi^+ e^+ e^-$ and $K^+ \rightarrow \pi^+ \mu^+ \mu^-$ decays are used as normalisation channels. The data sample corresponds to about 2.3×10^5 SPS spills. The typical beam intensity in 2017 was 2×10^{12} protons per SPS spill, equivalent to a mean beam particle rate at the FV entrance of about 500 MHz, and a mean K^+ decay rate in a 75 m-long FV of ~ 3.5 MHz.

The data sample used for this analysis has been collected with dedicated two-stage hardware (L0) and software (L1) trigger lines, enabled and run alongside the main $K^+ \rightarrow \pi^+ \nu \bar{\nu}$ line in a “parasitic” and non-interfering fashion. These trigger lines select multi-track, di-electron and di-muon final states. The former two lines are used to collect $K \rightarrow \pi e e$ candidates, and the latter line is used to collect $K \rightarrow \pi \mu \mu$ candidates. The low-level [10] (L0) multi-track trigger is based on RICH signal multiplicity and a requirement for a coincidence of signals in two opposite quadrants of a charge hodoscope. The di-electron L0 trigger additionally requires that at least 20 GeV of energy is deposited in the LKr calorimeter, while the di-muon L0 trigger requires a coincidence of signals

from two MUV3 tiles. The software (L1) trigger involves beam kaon identification by KTAG and reconstruction of a negatively charged track in STRAW. The multi-track, di-electron and di-muon trigger chains were downscaled typically by factors of 100, 8 and 2, respectively.

Both signal (LNV) and normalisation (SM) channels are collected concurrently, through the same trigger lines, and reconstructed from the same data sets. Under the assumption of similar kinematic distributions, this approach leads to first-order cancellation of effects due to trigger and detector inefficiencies, as well as event pileup. The SM $K^+ \rightarrow \pi^+ e^+ e^-$ and $K^+ \rightarrow \pi^+ \mu^+ \mu^-$ decays with $O(10^{-7})$ branching fractions are known experimentally to a few percent precision [11, 12]. The main steps of the $K^+ \rightarrow \pi^- e^+ e^+$ ($K^+ \rightarrow \pi^- \mu^+ \mu^+$) event selection are outlined:

- a good quality 3-track vertex with total charge +1 reconstructed in a fiducial decay volume defined as $105 \text{ m} < Z_{vtx} < 180 \text{ m}$ ($114 \text{ m} < Z_{vtx} < 180 \text{ m}$);
- track momenta selected in the range $8 \text{ GeV}/c < Z_{vtx} < 65 \text{ GeV}/c$ ($5 \text{ GeV}/c < Z_{vtx} < 65 \text{ GeV}/c$);
- three track times consistent within 15 ns (12 ns)
- the resultant 3-track momentum compatible with beam longitudinal and trasverse momenta (from nominal beam parameters);
- particle identification inferred through the reconstructed E/p ratio (energy deposited in LKr calorimeter divided by the track momentum measured by STRAW);

The latter E/p ratio is expected to be ~ 1 for e^\pm , almost null for minimum ionising particles like muons, and broadly distributed for pions (depending on the energy sharing between electromagnetic and hadronic shower components). For this analysis the following PID criteria have been used: $0.9 < E/p < 1.1$ for e^\pm , $E/p < 0.2$ for μ^\pm , and $E/p < 0.85$ for π^\pm . Muon candidates must have at least one MUV3 hit associated in time and space with the track reconstructed by the STRAW spectrometer. To reach the best sensitivity in the $K^+ \rightarrow \pi^- e^+ e^+$ analysis the RICH is also used for e^+ identification, exploiting the maximum likelihood fit probability to Cherenkov rings for different mass hypotheses. Furthermore, all photon veto detectors are applied to improve the background rejection from neutral pion decays (like Dalitz decay $\pi^0 \rightarrow e^+ e^- \gamma$).

4. Backgrounds

The main sources of background to $K^+ \rightarrow \pi^- e^+ e^+$ and $K^+ \rightarrow \pi^- \mu^+ \mu^+$ come from the $K^+ \rightarrow \pi^+ \pi^+ \pi^-$ channel, which is the dominant K^+ decay to three charged tracks, with a branching fraction of $B(K^+ \rightarrow \pi^+ \pi^+ \pi^-) = (5.583 \pm 0.024)\%$. The signal acceptances and the main backgrounds are evaluated using Monte Carlo (MC) simulations describing the detector geometry and response; input from data is used to tune and optimise several aspects of the simulations. Full data-driven methods are employed to address specific background sources.

Backgrounds to $K^+ \rightarrow \pi^- l^+ l^+$ occur via two main mechanisms: particle mis-identification (mis-ID); particle decays in flight. The π^\pm mis-identification as e^\pm (and viceversa) causes the main background contamination to $K^+ \rightarrow \pi^- e^+ e^+$ events. The estimate for this background is based on simulations involving the pion and electron identification efficiencies measured with data, as

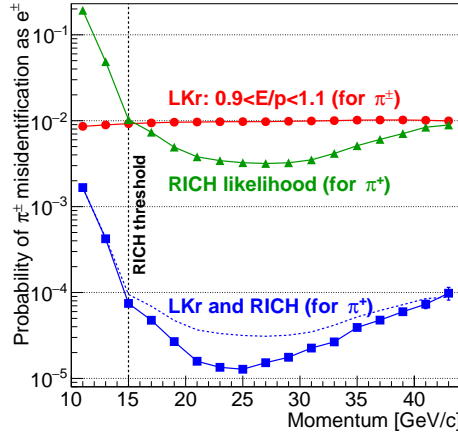


Figure 2: Measured probabilities of π^\pm mis-identification as e^\pm as functions of track momentum.

well as pion to electron (and electron to pion) mis-ID probabilities. Each quantity is measured as a function of the reconstructed track momentum using samples of pions and positrons, freed from background, from kinematic selections of $K^+ \rightarrow \pi^+ \pi^+ \pi^-$ and $K^+ \rightarrow e^+ \pi^0 \nu_e$. The LKr calorimeter response is known to be the same for electrons and positrons. All measured inefficiencies and mis-ID probabilities are at the level of 10^{-2} with weak momentum dependence; with the exception of the probability of π^\pm mis-ID as e^\pm , shown in Fig. 2. Different values are obtained using the LKr E/p condition alone (red), the RICH PID¹ alone (green), the multiplication of the two (blue, dashed), and the logical AND of the LKr and RICH (blue, solid). The combined probability reaches a minimum values of 10^{-5} for a momentum of 25 GeV/c, and increases up to 2×10^{-3} at 10 GeV/c, and to 10^{-4} at 45 GeV/c. The observed momentum dependence is due to the RICH Cherenkov threshold at low momentum, and the similarity of RICH response to e^+ and π^+ at high momentum.

Background contamination in the $K^+ \rightarrow \pi^- \mu^+ \mu^+$ sample is mainly due to $K^+ \rightarrow \pi^+ \pi^+ \pi^-$ processes with pion decays-in-flight to muons or pion mis-identified as muons. The latter is evaluated with the same technique as for $K^+ \rightarrow \pi^- e^+ e^+$, using simulations with inputs from dedicated studies based on control data samples. The former contamination, due to pion decays, can be accurately reproduced and the background estimate is based on special π^\pm decay enriched MC simulations. Pion decays in flight typically lead to reconstructed $\pi\mu\mu$ mass values well below the K^+ mass. However, depending on where the pion decays along the beam line, e.g. in the region between the STRAW magnet and the third chamber (or upstream the vacuum tank), effects like the mis-reconstruction of track momentum (or of the vertex kinematic properties) can give rise to high $\pi\mu\mu$ mass values contaminating the signal region. Background to $K^+ \rightarrow \pi^- \mu^+ \mu^+$ events due to $K^+ \rightarrow \pi^+ \pi^+ \pi^-$ decays with both π^+ mis-ID as μ^+ is estimated with data-driven methods, using a control sample collected with the multi-track trigger line. The full $K^+ \rightarrow \pi^- \mu^+ \mu^+$ event selection is applied, however the PID criteria are inverted to select $\pi\pi\pi$ vertices. The background contribution from $K^+ \rightarrow \pi^+ \pi^+ \pi^-$ decays with one π^+ decaying and another π^+ mis-ID as μ^+ is estimated in a similar way.

¹The RICH PID is only used for positrons.

5. Results

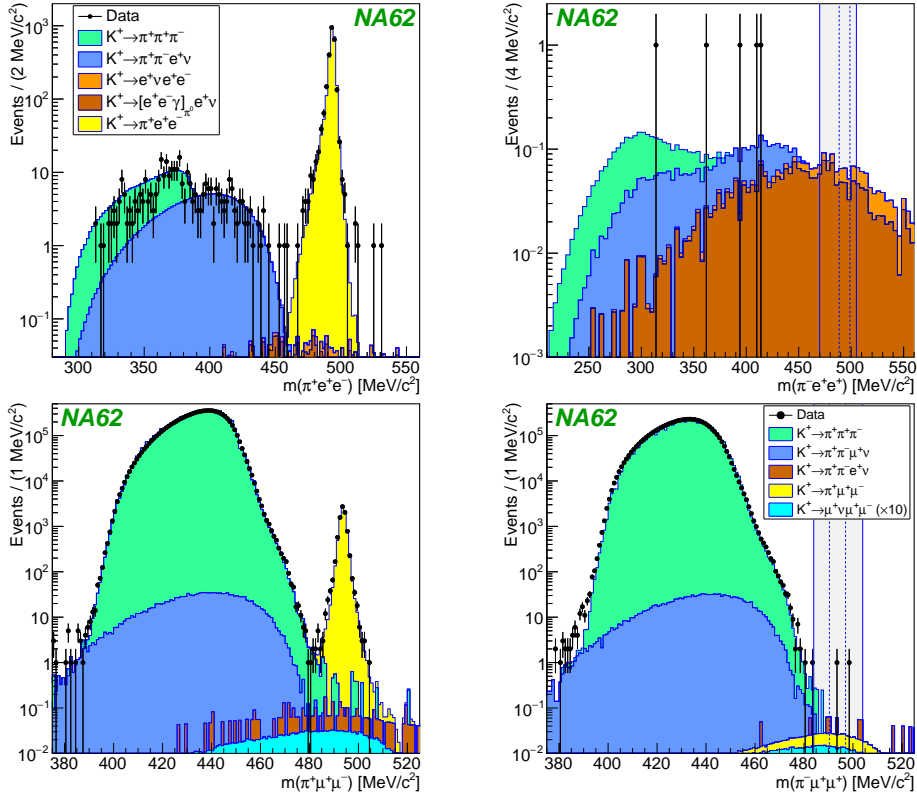


Figure 3: Reconstructed invariant πll mass spectra for selected samples of (top-left) SM $K^+ \rightarrow \pi^+ e^+ e^-$; (top-right) LNV $K^+ \rightarrow \pi^- e^+ e^+$; (bottom-left) SM $K^+ \rightarrow \pi^+ \mu^+ \mu^-$; (bottom-right) LNV $K^+ \rightarrow \pi^- \mu^+ \mu^-$. Data are overlaid with background estimates based on simulations. The shaded vertical bands indicate the regions masked during the analyses, which include the LNV signal regions bounded by dashed lines.

The final invariant mass $M(\pi ll)$ spectra for selected SM and LNV $K \rightarrow \pi ll$ (with $l = e, \mu$) candidates are shown in Fig. 3. The normalisation mode SM $K^+ \rightarrow \pi^+ e^+ e^-$ (Fig 3, top-left) is selected with a common event selection to the LNV mode (Fig 3, top-right), except for the charge and PID criteria. The event selection for $K^+ \rightarrow \pi^+ e^+ e^-$ includes the usage of RICH PID (for e^+ only). An auxiliary selection without RICH PID is used for the validation of background estimates. For the auxiliary selection the backgrounds in the control mass regions are simulated to few % relative precision, but the sensitivity to the LNV signal is limited by $K^+ \rightarrow \pi^+ \pi^0, \pi^0 \rightarrow e^+ e^- \gamma$ (with pi^+ mis-ID as e^+) background. Positron identification in the RICH leads to unprecedented background suppression for the selection of LNV $K^+ \rightarrow \pi^- e^+ e^+$ signal, thus improving its discovery potential. The overall background to the LNV signal is reduced by a factor of 6, with respect to the one obtained with the auxiliary analysis. In the SM signal mass region $470 \text{ MeV}/c^2 < M(\pi ee) < 505 \text{ MeV}/c^2$ (also masked region for the LNV mode) 2,484 $K^+ \rightarrow \pi^+ e^+ e^-$ candidates are observed with $M(ee) > 140 \text{ MeV}/c^2$. Using the world average $B(K^+ \rightarrow \pi^+ e^+ e^-) = (3.00 \pm 0.09) \times 10^{-7}$ [11], the number of K^+ decays in the fiducial volume is found to be: $N_K = (2.14 \pm 0.07) \times 10^{11}$. The signal acceptance for the LNV $K^+ \rightarrow \pi^- e^+ e^+$ decay (computed from simulations under the assumption of uniform phase-space) is 4.98%. A

single event sensitivity defined as $SES = \frac{1}{N_K \cdot A}$ of $(0.94 \pm 0.03) \times 10^{10}$ is obtained. The signal region for the LNV mode is defined as $(493.7 \pm 5.1) \text{ MeV}/c^2$, i.e. $(m(K^+) \pm (3 \times \sigma_{M(\pi ee)}))$. The total background estimate in the LNV $K^+ \rightarrow \pi^- e^+ e^+$ signal region is (0.16 ± 0.03) , where the error includes a systematic uncertainty of 15% in relative terms to account for the precision of the background description in the control mass regions when including the RICH PID. After unblinding no candidate events are observed in the LNV $K^+ \rightarrow \pi^- e^+ e^+$ signal region, and an upper limit is set on the branching fraction of the LNV mode using the CLs statistical treatment: $B(K^+ \rightarrow \pi^- e^+ e^+) < 2.2 \times 10^{-10}$ at 90% confidence level.

The RICH PID is not used in the selection of $K^+ \rightarrow \pi^- \mu^+ \mu^+$ events. So the normalisation SM $K^+ \rightarrow \pi^+ \mu^+ \mu^-$ mode (Fig 3, bottom-left) is selected with a common event selection to the LNV mode (Fig 3, bottom-right), except for the charge requirements. In the SM signal mass region $484 \text{ MeV}/c^2 < M(\pi ee) < 504 \text{ MeV}/c^2$ (also masked region for the LNV mode) 8,357 $K^+ \rightarrow \pi^+ \mu^+ \mu^-$ candidates are observed. Using the world average $B(K^+ \rightarrow \pi^+ \mu^+ \mu^-) = (0.962 \pm 0.025) \times 10^{-7}$ [12], the number of K^+ decays in the fiducial volume is found to be: $N_K = (7.94 \pm 0.23) \times 10^{11}$. The evaluated signal acceptance for the LNV mode is 9,81%. A single event sensitivity of $(1.28 \pm 0.04) \times 10^{10}$ is obtained. The signal region for the LNV mode is defined as $(493.7 \pm 3.3) \text{ MeV}/c^2$, i.e. $(m(K^+) \pm (3 \times \sigma_{M(\pi\mu\mu)}))$. The total background estimate in the LNV signal region is (0.91 ± 0.41) . The background description is validated by the agreement between the observed and predicted number of events in control mass regions, which is within 3% for both SM and LNV event selections. After unblinding 1 candidate event is observed in the LNV $K^+ \rightarrow \pi^- \mu^+ \mu^+$ signal region, and an upper limit is set on the branching ratio of the LNV mode using the CLs statistical treatment: $B(K^+ \rightarrow \pi^- \mu^+ \mu^+) < 4.2 \times 10^{-11}$ at 90% confidence level.

6. Conclusions

The NA62 experiment at CERN has a vast and unique physics programme including searches of LFV/LNV processes. Searches for LNV $K^+ \rightarrow \pi^- e^+ e^+$ and $K^+ \rightarrow \pi^- \mu^+ \mu^+$ decay, using a partial data set collected by NA62 in 2017 are reported. No signals are observed, but improved upper limits at 90% confidence level on the branching fractions of these decays are obtained: 2.2×10^{-10} and 4.2×10^{-11} , respectively. The sensitivities achieved are not limited by background, so further improvements are expected when using the full NA62 data set (about 3 times larger). With data collected in 2016-2018 NA62 has reached unprecedented sensitivities to branching fractions at the level of 10^{11} for a range of rare and forbidden K^+ decays. More analyses are ongoing and improvements with respect to world averages are expected for several LNV/LFV channels.

References

- | | |
|---|---|
| [1] L. S.Littenberg <i>et al.</i> , PLB 491 (2000) 285. | [7] G. Isidori <i>et al.</i> , EPJ C 77 (2017) 618. |
| [2] A. Atre <i>et al.</i> , JHEP 05 (2009) 030. | [8] E. Cortina Gil <i>et al.</i> , PLB 791 (2019) 156. |
| [3] R. Appel <i>et al.</i> , PRL 85 (2000) 2877. | [9] E. Cortina Gil <i>et al.</i> , JHEP 05 (2019) 182. |
| [4] R. J. Batley <i>et al.</i> , PLB 697 (2011) 107. | [10] R. Ammendola <i>et al.</i> , NIM A929 (2019) 1. |
| [5] E. Cortina <i>et al.</i> , JINST 12 (2017) P05025. | [11] J. R. Batley <i>et al.</i> , PLB 677 (2009) 246–254. |
| [6] M. Blanke <i>et al.</i> , EPJ C 76 (2016) 182. | [12] J. R. Batley <i>et al.</i> , PLB 697 (2011) 107–115. |